This is an open access article published under an ACS AuthorChoice License, which permits copying and redistribution of the article or any adaptations for non-commercial purposes.

ACS OMEGA

Article

Cite This: ACS Omega 2019, 4, 13538−13542

http://pubs.acs.org/journal/acsodf

# Effect of Structure on the Spin Switching and Magnetic Bistability of Solid-State Aryl Dicyanomethyl Monoradicals and Diradicals

Joshua P. Peterson, Rui Zhang, and Arthur H. Winter*

Department of Chemistry, Iowa State University, 1608 Gilman Hall, Ames, Iowa 50010, United States

Supporting Information

**ABSTRACT:** Stable organic radicals with switchable spin states have applications in medicine, biology, and material science. An emerging class of such spin-switchable radicals is based on dicyanomethyl radicals, which are typically thermally and air-stable species that form weakly bonded (closed-shell singlet) dimers at a lower temperature that rupture into electron paramagnetic resonance-active diradicals at a higher temperature. However, thus far, the study of these dicyanomethyl radicals has focused on their solution-phase behavior. An understanding of how chemical structure affects the solid-state spin switching behavior for these radicals is unknown. Here, we examine the solid-state spin crossover behavior of 6 monoradicals and 10 tethered diradicals and demonstrate that these species also undergo spin switching in the solid state. We find that the susceptibility for solid-state spin switching for the intermolecular dimers is weakly correlated to the solution-phase Gibbs free energies of dimerization, but no apparent correlations are seen between the solution-state free energies for the intramolecular dimerization and the solid-state behavior. Furthermore, intramolecular diradical dimers have greatly enhanced temperature-responsive behavior compared to their intermolecular counterparts. Crystalline and amorphous powders of the same radicals feature similar spin switching behavior, but the crystalline materials have slower bond-rupture kinetics at higher temperatures, suggesting that solid-state packing effects are an important kinetic consideration. An interesting feature of these systems is that, upon cooling down to room temperature after heating, some radicals remain trapped in the solids, indicating magnetic bistability, while others partially or fully return to the diamagnetic dimers. This work provides insights into how chemical structure affects spin crossover in the solid state for this new class of air-stable radicals, the knowledge of importance for the construction of dynamically responsive solid-state materials, and organic spin crossover polymers.

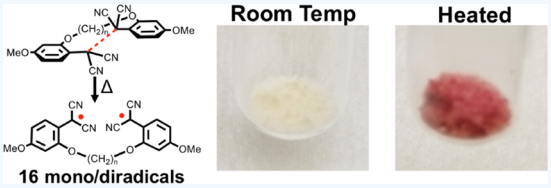


## INTRODUCTION

Organic radicals with switchable spin states are emerging materials with applications in turn-on magnetic resonance contrast reagents, spintronics, dynamic covalent assemblies, and stimuli-responsive polymers and plastics.[1−5] Such spin-switchable materials undergo a change in spin state in response to external stimuli or environmental cues. Switching between the standard properties of closed-shell molecules to spin-unpaired radicals leads to large changes in the optical, magnetic, and conductivity properties of these materials with relatively mild external stimuli, making this spin switching strategy an attractive one for the design of stimuli-responsive materials.

A critical barrier toward the development of such spin crossover organic materials is the requirement for stable organic radicals that can switch between spin states. Regrettably, most stable organic radicals do not show such spin switching behavior. However, dicyanomethyl radicals have recently been demonstrated as promising building blocks for such spin-switchable materials because they are air- and thermally stable species and can switch between weakly bonded closed-shell forms and spin-unpaired forms.[6−10] Furthermore, the strength of the spin−spin interaction can be tuned by substituents.[6] The nature of the spin−spin interaction for these dicyanomethyl radicals is typically a very weak sigma dimer (with a C−C distance >1.6 A) or an antiferromagnetically spin-coupled pi dimer. There are cases of organic radicals investigated in the solid state;[11−16] however, detailed studies of dicyanomethyl organic radicals have been mostly limited to the solution phase.

To understand how the structure affects spin crossover in the solid state, here, we report a study of a family of dicyanomethyl monoradicals and tethered diradicals using variable-temperature electron paramagnetic resonance (EPR), allowing the comparison of the solid-state behavior of 6 monoradicals and 10 tethered diradicals (Figure 1) to their previously reported solution-phase behavior.

## RESULTS AND DISCUSSION

All of the monoradicals and linked diradicals (shown in Figure 1) in this study exhibit qualitatively similar temperature-responsive behavior in the solid state. At low temperatures, either no EPR signal or a very small one is observed. In all cases, an EPR signal grows in as the temperature is increased. This increase in the EPR signal is accompanied by a color change in the solid from typically a light powder to a darkly

Received: June 24, 2019
Accepted: July 29, 2019
Published: August 9, 2019

Downloaded via IOWA STATE UNIV on June 30, 2020 at 18:30:39 (UTC).
See https://pubs.acs.org/sharingguidelines for options on how to legitimately share published articles.

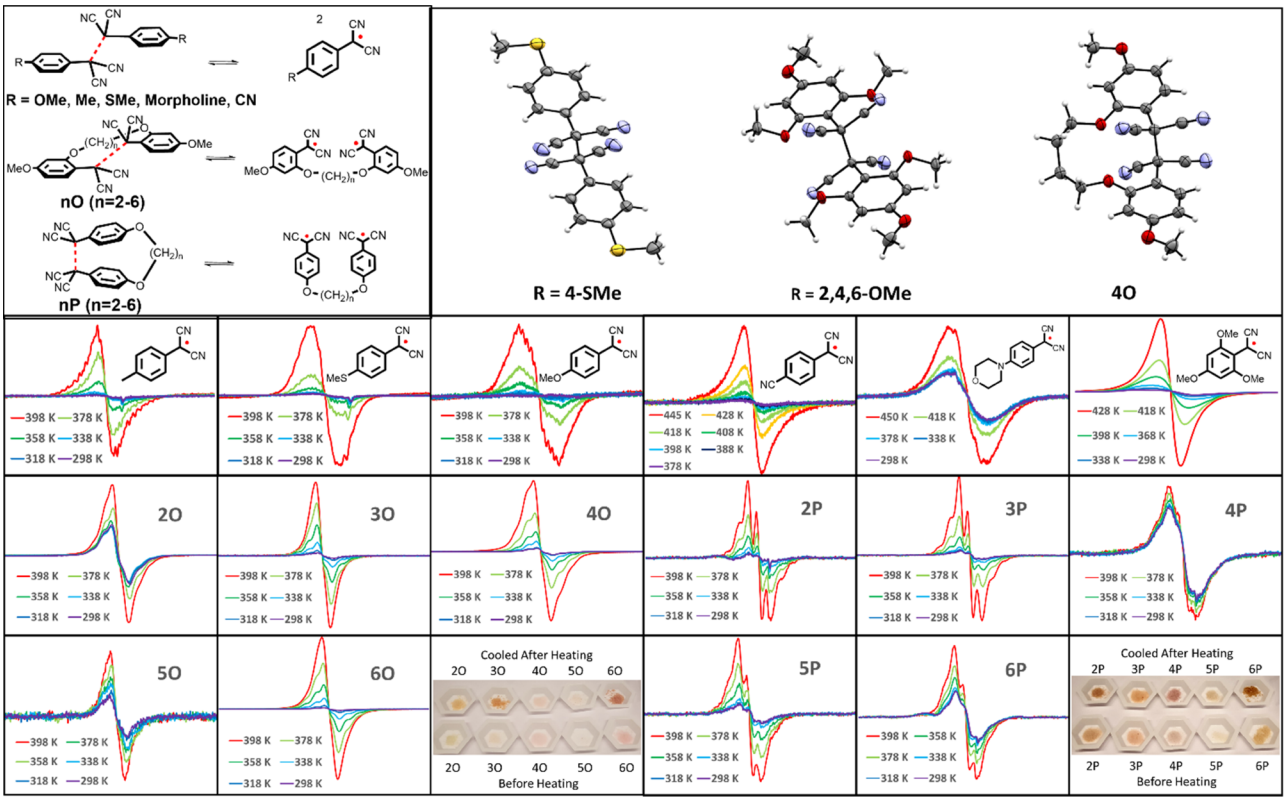


**Figure 1.** Radical−dimer equilibria for all subsets of compounds (top left); crystal structure for thiomethyl, trimethoxy (reproduced from ref 7), and 4O dimers (top right) (reproduced from ref 7); and all VT-EPR data for the 16 solid-state samples in this work (bottom).

colored one (see the movie in the Supporting Information (SI)). Except where noted, after a brief temperature equilibration period, the EPR signal is stable. These features are consistent with rupturing of the colorless sigma dimers into their colored diradical forms as the temperature is increased, similar to their solution-phase behavior.

**Correlation between Solution-Phase Radical Dimerization $K_a$ and Solid-State Radical Behavior.** We were interested in whether there is a correlation between the solution-phase equilibrium constants for the radicals and the corresponding solid-state spin switching behavior. Intuitively, one expects radicals with weaker bonding interactions in the solution phase to have a higher susceptibility for solid-state spin crossover. To test this hypothesis, we evaluated six monoradicals with varying para substituents (OMe, Me, SMe, morpholine, CN, and 2,4,6-OMe) that have varying solution-phase $K_a$ values for dimerization. Radicals featuring donating substituents appended to the aryl ring have lower solution-phase $K_a$ values for dimerization, while those with withdrawing groups (e.g., CN) have a stronger interaction. A Hammett plot of the $\sigma^+$ of the para substituent vs the $K_a$ shows a positive correlation.[6]

Indeed, a comparison of the solution-state $K_a$ values vs the sample spin count observed at 398 K shows a negative correlation (see SI Figure S4). The 2,4,6-trimethoxy monoradical, which has the lowest binding constant ($1.9 \times 10^5$ $M^{-1}$), has the highest percentage of spins, while the *p*-cyano derivative, which has the highest solution binding constant ($1.8 \times 10^8$ $M^{-1}$), has the lowest percentage of spins. In general, however, the spin count observed for the solid monoradicals is orders of magnitude lower than the spin count observed in solution from 3 to 5 mM measured at the same temperature.

For the intramolecular dimers, however, the spin count is about 2 orders of magnitude higher in the solid state than for the monoradicals, and in some cases, it is higher than that observed for the same diradicals in solution. For example (see Figure 2), **4O**, **3P**, and **4P** show a greater spin count in the solid state than in solution at all temperatures studied. However, for these intramolecular diradical cases, there is no discernible correlation between the intramolecular $K_a$ determined in solution and the solid-state spin switching behavior. Indeed, in the solid state, the temperature-responsive spin switching curves are all relatively similar, despite differences in the solution $K_a$ between these linked diradicals. Given that the primary difference in these linked diradicals is the linker length, which leads to large changes in solution-phase entropy, this is perhaps not so surprising because in solution, the diradical is free to sample conformational space, which is not the case in the confined solid-state environment. Thus, the differences are larger in the solution state for these tethered diradicals than in the solid state.

**Reversibility of Spin Crossover.** A major difference between solution-state and solid-state spin crossovers is the reversibility of spin crossover. In solution, rapid equilibration ensures a Boltzmann population of spin-paired and spin-unpaired species. Upon lowering the temperature, radicals immediately return to the dimers. In contrast, we find that in the solid state, some of the radicals show magnetic bistability (e.g., stay trapped in the paramagnetic state) despite lowering the temperature.

After performing variable-temperature EPR on the ortho and para tethered diradicals, we evaluated the ability of the samples



DOI: 10.1021/acsomega.9b01658
ACS Omega 2019, 4, 13538−13542

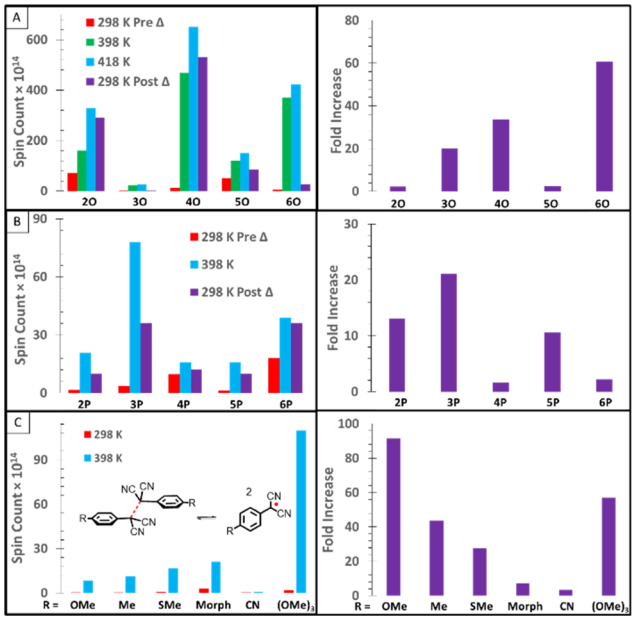


**Figure 2.** Spin counts at various temperatures for ortho tethers (A), para tethers (B), and monoradicals (C) with fold increases from 298 to 398 K to the right of each.

to return back to their diamagnetic dimers upon cooling. In solution, all compounds return completely to their starting equilibrium spin concentration upon cooling and can be reversibly cycled. This is not so in the solid state (see Figure 2). Some of the tethered diradicals tested here in the solid state show increases in radical concentration at elevated temperatures, but upon cooling, the radical concentrations remained elevated for over 12 months of extended sitting under air (evidenced by the after-heated pictures in Figure 1). Examples of this type include **2O**, **4O**, and **6P**. Others (e.g., **2P**, **3P**, **5P**, **5O**) show a partial return. In still other cases (e.g., **3O**, **6O**), we observed a nearly complete return to the starting radical concentration upon cooling.

**Difference between Crystalline and Amorphous Materials.** The samples tested in Figure 1 are amorphous powders. We asked the question of whether there would be a difference in the spin switching behavior if the samples were crystalline solids. For two of the monoradicals, we obtained sufficient quantities of X-ray quality single crystals of the materials (see Figure 1) to perform solid-state VT-EPR measurements. In these two cases, we compared the temperature-responsive behavior of the amorphous powders compared to that of the single crystals (see Figure 3). The most striking difference is that, at higher temperatures, the crystalline compound shows further growth in the EPR signal over time after our short-temperature equilibration in the EPR cavity, while the amorphous samples do not show any further increase in their EPR signal. Essentially, the compound does not reach a quick equilibrium at elevated temperatures and the radical continues to form slowly over time. In the case of the *p*-thiomethyl monoradical, the further increase is substantial. Thus, the kinetics of bond rupture appear to be altered by solid-state morphology, and there appears to be a barrier for spin crossover in crystalline materials not present in the amorphous solids.

By analyzing the combined data (i.e., spin counts at various temperatures) for all 16 compounds (Figure 2), some interesting trends were observed. Compounds **4O** and **6O** showed largest increases for those diradicals substituted at the ortho position, while **3P** and **5P** show the largest increase in the spin count for the para-substituted diradical series. Compound **2P** is much less flexible than other compounds, and we hypothesize that it behaves differently because of this. An alternative possibility is that some of these diradicals form higher-order aggregates (dimer, trimer, oligomer, etc.) in the solid state. In the nontethered series, the donating ability of each substituent correlated well with the fold increase in the amount from 398 to 298 K with the exception of the morpholine substitute compound. As noted in our previous work, the para-nitrogen-containing dicyanomethyl radicals can suffer decomposition at elevated temperatures, and this also occurred in the solid state for this radical.

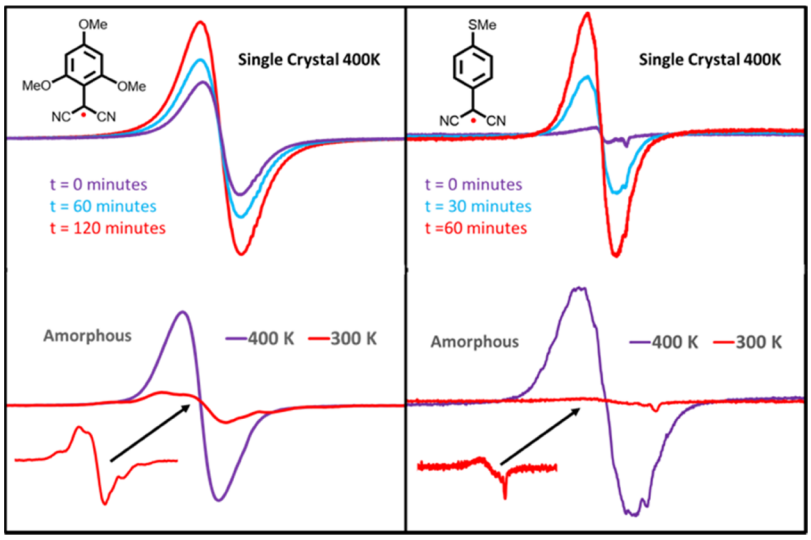


**Figure 3.** Single-crystal EPR data at 400 K for 2,4,6-trimethoxy- and *p*-thiomethyl-substituted dimers with amorphous powder EPR spectra for each compound below.



DOI: 10.1021/acsomega.9b01658
*ACS Omega* 2019, 4, 13538−13542

## CONCLUSIONS

In conclusion, we have investigated the effect of structure on the spin crossover behavior of a family of dicyanomethyl monoradicals and linked diradicals. All radicals and diradicals show a 10- to 100-fold increase in spin counts upon being heated, with the linked diradicals being much more susceptible to spin crossover than the monoradicals. For the monoradicals, the solution-state $K_a$ correlates weakly with the solid-state spin switching behavior, but there is no correlation for the linked dimers, which all show similar behavior due to a reduction of the importance of conformational entropy in the solid state. The kinetics of spin crossover differ between crystalline samples and amorphous powders, suggesting the importance of crystal packing and hinting at cooperative effects. The reversibility of spin crossover varies greatly among the radical structures, with some powders trapping the radicals generated upon heating and showing magnetic bistability, while others showing either partially or fully reversible behavior. These studies with discrete well-defined radicals lay the groundwork for using these radicals and diradicals as the building blocks for stimuli-responsive spin crossover polymers and bulk materials.

## EXPERIMENTAL SECTION

**General Procedure in the Preparation of Amorphous Powder Solid-State EPR Experiments.** All of the compounds in this paper, the 6 intermolecular dimers and the 10 tethered intramolecular dimers, were all synthesized according to previous reports by our lab.[6,7] At the time for each experiment, a fresh sample of each compound was oxidized from the precursor −CH adduct to generate the radical/dimer species. Upon workup for these oxidations, during solvent removal of the purification step, freshly purified potassium chloride salt was added to the mixture to make an even dispersion in the sample tube. When all solvents were removed, the desired compounds were then mixed with KCl salt and finely ground using a mortar and pestle. Compounds were added to EPR tubes and then sealed under normal atmospheric conditions. The ratio of KCl to compound in question was kept constant in all samples for consistency. A known weight of oxidized compound contained within the EPR window was calculated for spin count calculations. After EPR experiments, all samples were saved and placed into vials for future experiments because these compounds do not decompose over time, as evidenced by investigating samples many months after initial oxidation and EPR study. Compounds tested in the solid state can be dissolved and analyzed in solution to yield the exact same data from our previously published papers. This is also useful because it allows a "reset" to the dimer after spin switching to the diradical in the solid state, some of which is not reversible.

**General Procedure in the Preparation of Single-Crystal Solid-State EPR Experiments.** For the 2,4,6-trimethoxy- and thiomethyl-substituted compounds, sufficient amounts of single crystals were formed to allow for direct EPR characterization on the single crystals themselves. Crystals were grown by slow evaporation of compounds dissolved in toluene; this process occurred serendipitously over the course of a few months after initial solution EPR experiments. Single crystals were carefully added with a spatula to a 3 mm EPR tube, and the tube was sealed under atmospheric conditions. For the longer kinetic scans on the crystals, a built-in kinetics parameter on the instrument allowed for scanning the sample over a long period of time at various time increments while at the elevated temperature.

**EPR Instrument Parameters.** The following parameters were used on the EPR instrument for variable-temperature acquisitions: modulation frequency, 100 kHz; receiver gain, 50 dB; modulation amplitude, 0.5−1 G; time constant, 0.1 s; center field, 3330 G; sweep width, 300 G; microwave attenuation, 20 dB; microwave power, 2 mW; number of data points, 2048. For the determination of spin count, a calibration curve was generated using a sample of TEMPO at various concentrations.

## MATERIALS AND METHODS

**Variable-Temperature EPR Experiments.** Variable-temperature EPR studies were performed on all compounds, radicals and diradicals, to elucidate the effect of temperature on the homolytic bond cleavage to generate each, in the solid state. All compounds were investigated in the solid state, with a portion of each sample, ranging from 5 to 10 mg, in a sealed quartz EPR tube. During experiments on the EPR spectrometer, a spectrum was recorded at 10 K intervals after allowing 5 min for the sample to reach an equilibrated temperature. The temperature range for each sample was from 298 to 418 K at minimum; some samples were investigated at even higher temperatures up to 450 K. Follow-up EPR scans were performed after the samples were cooled back to room temperature to gauge the reversibility for each sample to return to starting temperature radical concentrations.

## ASSOCIATED CONTENT

### Supporting Information

The Supporting Information is available free of charge on the ACS Publications website at DOI: 10.1021/acsomega.9b01658.

Methoxy substituted solid with heat gun (MP4)

X-ray crystallographic data: procedures for sample prep, EPR characterization parameters, kinetics plots, and comparison graphs (CIF)

Graphs of radical percentages for solid and solution data; plot of $K_a$ vs 398 K solid state radicals; ellipsoid plot of R = SMe intramolecular dimer with refinement data; kinetics plots of high temp crystals (PDF)

## AUTHOR INFORMATION


### Corresponding Author

*E-mail: winter@iastate.edu.

### ORCID

Joshua P. Peterson: 0000-0002-9897-238X

Arthur H. Winter: 0000-0003-2421-5578



### Funding

Financial support from NSF (CHE-1764235) and the ISU Bailey research award is gratefully acknowledged.


### Notes

The authors declare no competing financial interest.

## ACKNOWLEDGMENTS

The authors thank Dr Sarah Cady and the Chemical Instrumentation Facility at Iowa State for assistance with variable-temperature EPR acquisition.



DOI: 10.1021/acsomega.9b01658
ACS Omega 2019, 4, 13538−13542

## REFERENCES


(1) Grossel, M. C.; Weston, S. C. Synthesis of materials for molecular electronic applications. *Contemp. Org. Synth.* **1994**, *1*, 367−386.

(2) Hughes, B. K.; Braunecker, W. A.; Bobela, D. C.; Nanayakkara, S. U.; Reid, O. G.; Johnson, J. C. Covalently Bound Nitroxyl Radicals in an Organic Framework. *J. Phys. Chem. Lett.* **2016**, *7*, 3660−3665.

(3) Li, L. H.; Feng, X. L.; Cui, X. H.; Ma, Y. X.; Ding, S. Y.; Wang, W. Salen-Based Covalent Organic Framework. *J. Am. Chem. Soc.* **2017**, *139*, 6042−6045.

(4) Ma, Y. X.; Li, Z. J.; Wei, L.; Ding, S. Y.; Zhang, Y. B.; Wang, W. A Dynamic Three-Dimensional Covalent Organic Framework. *J. Am. Chem. Soc.* **2017**, *139*, 4995−4998.

(5) Montoro, C.; Rodríguez-San-Miguel, D.; Polo, E.; Escudero-Cid, R.; Ruiz-González, M. L.; Navarro, J. A. R.; Ocón, P.; Zamora, F. Ionic Conductivity and Potential Application for Fuel Cell of a Modified Imine-Based Covalent Organic Framework. *J. Am. Chem. Soc.* **2017**, *139*, 10079−10086.

(6) Peterson, J. P.; Geraskina, M. R.; Zhang, R.; Winter, A. H. Effect of Substituents on the Bond Strength of Air-Stable Dicyanomethyl Radical Thermochromes. *J. Org. Chem.* **2017**, *82*, 6497−6501.

(7) Zhang, R.; Peterson, J. P.; Fischer, L. J.; Ellern, A.; Winter, A. H. Effect of Structure on the Spin−Spin Interactions of Tethered Dicyanomethyl Diradicals. *J. Am. Chem. Soc.* **2018**, *140*, 14308−14313.

(8) Kobashi, T.; Sakamaki, D.; Seki, S. N-Substituted Dicyanomethylphenyl Radicals: Dynamic Covalent Properties and Formation of Stimuli-Responsive Cyclophanes by Self-Assembly. *Angew. Chem., Int. Ed.* **2016**, *55*, 8634−8638.

(9) Okino, K.; Hira, S.; Inoue, Y.; Sakamaki, D.; Seki, S. The Divergent Dimerization Behavior of N-Substituted Dicyanomethyl Radicals: Dynamically Stabilized versus Stable Radicals. *Angew. Chem., Int. Ed.* **2017**, *129*, 16824−16828.

(10) Hartzler, H. D. Polycyano Radicals. *J. Org. Chem.* **1966**, *31*, 2654−2658.

(11) Hicks, R. G. A new spin on bistability. *Nat. Chem.* **2011**, *3*, 189.

(12) Bag, P.; Pal, S. K.; Itkis, M. E.; Sarkar, A.; Tham, F. S.; Donnadieu, B.; Haddon, R. C. Synthesis of Tetrachalcogenide-Substituted Phenalenyl Derivatives: Preparation and Solid-State Characterization of Bis(3,4,6,7-tetrathioalkyl-phenalenyl)boron Radicals. *J. Am. Chem. Soc.* **2013**, *135*, 12936−12939.

(13) Leitch, A. A.; Lekin, K.; Winter, S. M.; Downie, L. E.; Tsuruda, H.; Tse, J. S.; Mito, M.; Desgreniers, S.; Dube, P. A.; Zhang, S.; Liu, Q.; Jin, C.; Ohishi, Y.; Oakley, R. T. From Magnets to Metals: The Response of Tetragonal Bisdiselenazolyl Radicals to Pressure. *J. Am. Chem. Soc.* **2011**, *133*, 6051−6060.

(14) Morita, Y.; Suzuki, S.; Fukui, K.; Nakazawa, S.; Kitagawa, H.; Kishida, H.; Okamoto, H.; Naito, A.; Sekine, A.; Ohashi, Y.; Shiro, M.; Sasaki, K.; Shiomi, D.; Sato, K.; Takui, T.; Nakasuji, K. Thermochromism in an organic crystal based on the coexistence of $\sigma$- and $\pi$-dimers. *Nat. Mater.* **2008**, *7*, 48.

(15) Sarkar, A.; Pal, S. K.; Itkis, M. E.; Tham, F. S.; Haddon, R. C. Sulfur and selenium substituted spiro-biphenalenyl-boron neutral radicals. *J. Mater. Chem.* **2012**, *22*, 8245−8256.

(16) Fourmigué, M.; Lieffrig, J. Organizing radical species in the solid state with halogen bonding. *Top. Curr. Chem.* **2015**, *359*, 91−113.




DOI: 10.1021/acsomega.9b01658
*ACS Omega* 2019, 4, 13538−13542